

---

# NONPARAMETRIC STOCHASTIC SUBSPACES VIA THE BOOTSTRAP FOR CHARACTERIZING MODEL ERROR

---

**Akash Yadav**  
University of Houston  
ayadav4@uh.edu

**Ruda Zhang**  
University of Houston  
rudaz@uh.edu

## ABSTRACT

Reliable forward uncertainty quantification in engineering requires methods that account for aleatory and epistemic uncertainties. In many applications, epistemic effects arising from uncertain parameters and model form dominate prediction error and strongly influence engineering decisions. Because distinguishing and representing each source separately is often infeasible, their combined effect is typically analyzed using a unified model-error framework. Model error directly affects model credibility and predictive reliability; yet its characterization remains challenging. To address this need, we introduce a bootstrap-based stochastic subspace model for characterizing model error in the stochastic reduced-order modeling framework. Given a snapshot matrix of state vectors, the method leverages the empirical data distribution to induce a sampling distribution over principal subspaces for reduced order modeling. The resulting stochastic model enables improved characterization of model error in computational mechanics compared with existing approaches. The method offers several advantages: (1) it is assumption-free and leverages the empirical data distribution; (2) it enforces linear constraints (such as boundary conditions) by construction; (3) it requires only one hyperparameter, significantly simplifying the training process; and (4) its algorithm is straightforward to implement. We evaluate the method's performance against existing approaches using numerical examples in computational mechanics and structural dynamics.

**Keywords** Model error · Model-form uncertainty · Stochastic reduced-order modeling · Bootstrap · Non-parametric method

## 1 Introduction

Engineering systems often exhibit uncertainty, which may arise from various sources, including the intrinsic variability of the system and incomplete knowledge of the governing physics. In the context of uncertainty quantification (UQ), these are commonly categorized into aleatory and epistemic uncertainties. *Aleatory* uncertainty stems from intrinsic variability in systems and data, such as fluctuating boundary conditions, imprecise material properties, environmental conditions, or measurement noise, and is often irreducible (Kiureghian and Ditlevsen, 2009). *Epistemic* uncertainty

results from incomplete knowledge, modeling assumptions, and numerical approximations; unlike aleatory uncertainty, it can in principle be reduced with deeper physical understanding, improved models, or additional data (Oberkampf et al., 2002; Roy and Oberkampf, 2011).

Within epistemic uncertainty, multiple sources such as uncertain inputs, parameters, and model form typically coexist. Errors in model parameters and model form are often intertwined; a practical and widely used perspective is to analyze their combined effect through a unified *model-error* framework. Model error refers to the discrepancy between model predictions and ground truth; in various contexts, it is also called model inadequacy, model discrepancy (Kennedy and O'Hagan, 2001), or structural uncertainty (Trucano et al., 2006). It arises when the numerical model fails to accurately capture the behavior of the true system, resulting in a systematic prediction error (i.e., model error) that extends beyond parametric misspecification. Treating model-form uncertainty as parametric uncertainty can lead to biased and overconfident predictions (Arendt et al., 2012; Tuo and Jeff Wu, 2016; Pernot, 2017). Model error is often a key factor in epistemic uncertainty, but it is a challenging problem. Model error analysis is typically divided into two components: characterization and correction. *Characterization* refers to quantifying the predictive error of an inadequate model, whereas *correction* involves reducing the predictive error of an inadequate model via some form of adjustment. Works on this topic often provide probabilistic representations of model error, which can be categorized into parametric and nonparametric approaches.

*Parametric approaches* employ a statistical model that specifies a family of distributions with a fixed, finite number of parameters. In model-error analysis, such parameterizations are attractive because they typically yield tractable inference. Representative examples include stochastic closure models in governing equations, and parametric representations of discrepancy in numerical models and surrogate models. Xiao et al. (2016) present a data-driven physics-informed Bayesian framework based on an iterative ensemble Kalman method to assimilate prior knowledge and observation data for quantifying and reducing model-form uncertainties in Reynolds-averaged Navier-Stokes simulations. Morrison et al. (2018) address model inadequacy with stochastic operators introduced as a source in the governing equations while preserving underlying physical constraints. Similarly, Portone and Moser (2022) propose a stochastic operator for an unclosed dispersion term in an averaged advection-diffusion equation for model closure. Sargsyan et al. (2019) provide a Bayesian framework with embedded model error using polynomial chaos expansions (PCEs) for improved uncertainty representation in computational models. Wang and Ghanem (2023) introduce a Bayesian parametric model for statistical calibration of model error induced by uncertainty in PCE coefficients. Zou et al. (2024) present a method for correcting model misspecification in physics-informed neural networks (PINNs) using Bayesian PINNs and ensemble PINNs. Parametric model-error formulations span a broad literature, and these works are intended as an illustrative sample.

*Nonparametric approaches* do not restrict the data-generating mechanism to a fixed finite-dimensional form: the unknown object is either infinite-dimensional or its effective dimension grows with the data. Nonparametric methods are flexible and robust to model misspecification, but they can be challenging to use for inference and computation; consequently, relatively few methods fall into this category. One of the earliest nonparametric approaches for model error is the Kennedy-O'Hagan (KOH) framework, which corrects model error by learning a Gaussian process (GP) discrepancy from data, providing a flexible representation without prescribing a fixed form (Kennedy and O'Hagan, 2001). Despite its wide adoption (Higdon et al., 2004, 2008; Qian and Wu, 2008), the KOH framework can exhibit identifiability issues between calibration parameters and discrepancy and may extrapolate unreliably without informative priors or physics-based structure

(Strong and Oakley, 2014; Brynjarsdóttir and O’Hagan, 2014; Sargsyan et al., 2015; Plumlee, 2017; Maupin and Swiler, 2020). Beyond output-discrepancy models, some nonparametric strategies place GPs directly on operators and fields. For example, Girolami et al. (2021) model the forcing term and the coefficients of the differential equation as GPs and develop a statistical finite element method that coherently synthesizes observation data and model predictions. Yet it is challenging to scale this approach to high-dimensional problems.

A recent nonparametric model (NPM) for model uncertainty (Soize and Farhat, 2017) merges projection-based reduced-order modeling with random matrix theory. This framework uses randomized a reduced-order basis (ROB) to induce a stochastic reduced-order model (ROM), which allows efficient characterization of model error as it involves computationally inexpensive ROMs instead of full-order models. The stochastic ROBs used in the NPM are defined through a sampling procedure: samples from a Gaussian process are stacked into a matrix, and boundary conditions are explicitly enforced; the matrix is then used to construct a perturbed version of the deterministic ROB through tangential projection and polar decomposition. Hyperparameters of the stochastic ROB are identified by solving a reduced statistical inverse problem. The NPM method has been applied to various engineering problems (Wang et al., 2019; Soize and Farhat, 2019), with recent efforts focused on reducing the number of hyperparameters and simplifying training (Soize and Farhat, 2019; Azzi et al., 2022).

Following the stochastic ROM framework but designed for multi-model settings, the Riemannian stochastic model (RSM) (Zhang and Guilleminot, 2023) works with a different set of stochastic basis: a Dirichlet distribution anchored to the candidate models’ ROBs is constructed on a tangent space of the Stiefel manifold, and its samples are reconstructed as bases via the Riemannian exponential map. The RSM estimates its hyperparameters by solving a quadratic program and has been applied in computational mechanics (Zhang et al., 2024; Quek et al., 2025).

In prior work, we introduced SS-PPCA, which models principal subspaces via probabilistic PCA (Yadav and Zhang, 2025b). Also based on a stochastic ROM framework, SS-PPCA differs from NPM and RSM in its modeling approaches: NPM and RSM model stochastic ROBs, whereas SS-PPCA models the subspaces directly. SS-PPCA provides analytical distributions for the associated random matrices and subspaces and involves only a single hyperparameter, which simplifies both its implementation and training. However, it relies on a Gaussian latent variable model, which, while often effective, may not perform well for heavy-tailed, skewed, or multimodal data.

In this paper, we present a nonparametric, data-driven framework—stochastic subspace via bootstrap (SS-Bootstrap)—for probabilistic modeling of principal subspaces and characterization of model error. Unlike SS-PPCA, which relies on a Gaussian latent-variable structure, SS-Bootstrap operates directly on the empirical data distribution via resampling, leveraging classical bootstrap principles (Efron, 1979; Efron and Tibshirani, 1994). This makes the framework broadly applicable, assumption-light, and naturally robust to non-Gaussian and multimodal data. The main contributions of our work are as follows:

1. We propose a novel non-parametric, data-driven framework for stochastic subspace modeling based on bootstrap resampling, which is simple, distribution-free, and computationally efficient.
2. We use this stochastic subspace model to construct stochastic ROMs with a single scalar hyperparameter. This contrasts with existing stochastic ROM approaches, which use stochastic bases and typically involve more hyperparameters.

3. We demonstrate, through a series of numerical experiments, that our method provides consistent and sharp uncertainty estimates with a low computational cost.

The remainder of the paper is organized as follows. [Section 2](#) reviews stochastic reduced-order modeling. [Section 3](#) presents the proposed stochastic subspace model, sampling algorithm, and strategy for hyperparameter optimization. [Section 4](#) reviews related work. [Section 5](#) validates the proposed method through numerical examples. Finally, [Section 6](#) concludes with a summary and directions for future work.

*Notation.* Throughout this paper, vectors are denoted by bold lowercase letters (e.g.,  $\mathbf{x}$ ), matrices by bold uppercase letters (e.g.,  $\mathbf{X}$ ), and scalars by regular typeface (e.g.,  $x_i$ ). Subspaces are denoted by calligraphic uppercase letters (e.g.,  $\mathcal{V}$ ). Random quantities share the same notation as their deterministic counterparts; their nature should be clear from the context.

## 2 Stochastic reduced-order modeling

This section develops the formulation of stochastic reduced-order models (SROMs). We first define the high-dimensional model (HDM), then construct a deterministic reduced-order model (ROM) from the HDM, and finally formulate an SROM based on the ROM. The presentation is kept general so that the framework applies across a broad range of physical and engineering systems.

### 2.1 High-dimensional model

Consider a parametric nonlinear dynamical system governed by a set of ordinary differential equations (ODEs):

$$\dot{\mathbf{x}} = \mathbf{f}(\mathbf{x}, t; \boldsymbol{\mu}), \quad (1)$$

where  $\mathbf{x} \in \mathbb{R}^n$  is the state vector,  $t \in [0, \infty)$  is time, and  $\boldsymbol{\mu}$  denotes the parameter vector. The initial condition is  $\mathbf{x}(0) = \mathbf{x}_0$ , and the system is subject to linear constraints of the form  $\mathbf{B}^\top \mathbf{x} = 0$ , with  $\mathbf{B} \in \mathbb{R}^{n \times n_{CD}}$ . These constraints often encode boundary conditions. Nonhomogeneous linear constraints can be recast as homogeneous ones by a state shift, without loss of generality. Such systems typically arise from the spatial discretization of partial differential equations governing physical processes, resulting in *high-dimensional models* (HDMs) with  $n \gg 1$ . For steady-state problems, [Eq. \(1\)](#) reduces to an algebraic system  $\mathbf{f}(\mathbf{x}; \boldsymbol{\mu}) = 0$ . The HDM is an approximation of the physical system due to modeling and numerical assumptions; the resulting discrepancy is the target for model-error analysis.

### 2.2 Reduced-order model

Reduced-order models (ROMs) can be constructed from the HDM to accelerate simulations while maintaining accuracy. A standard approach for ROM construction is the Galerkin projection, which projects the HDM orthogonally onto a  $k$ -dim subspace  $\mathcal{V}$  of the state space  $\mathbb{R}^n$ . This reduced subspace  $\mathcal{V}$  can be obtained, for example, using proper orthogonal decomposition (POD) ([Sirovich, 1987](#)) applied to a snapshot matrix of HDM solutions, or from the eigendecomposition of the system operators ([Chopra, 1996](#)). For POD, the reduced order  $k$  is typically selected to meet a prescribed energy threshold retained by the POD modes. Let  $\mathbf{V} \in \text{St}(n, k)$  be an orthonormal basis of the subspace  $\mathcal{V}$ , then the ROM can be written as:

$$\mathbf{x} = \mathbf{V}\mathbf{q}, \quad \dot{\mathbf{q}} = \mathbf{V}^\top \mathbf{f}(\mathbf{V}\mathbf{q}, t; \boldsymbol{\mu}), \quad (2)$$

with reduced coordinates  $\mathbf{q} \in \mathbb{R}^k$  and initial conditions  $\mathbf{q}(0) = \mathbf{V}^\top \mathbf{x}_0$ . To satisfy the linear constraints, we must have  $\mathbf{B}^\top \mathbf{V} = 0$ . Since POD bases are constructed from snapshot data, the resulting ROM automatically satisfies any linear constraints (homogeneous or non-homogeneous) present in the snapshots. In steady-state setting, Eq. (2) reduces to a set of algebraic equations:  $\mathbf{V}^\top \mathbf{f}(\mathbf{V}\mathbf{q}; \boldsymbol{\mu}) = 0$ . Although ROMs offer substantial computational savings, they introduce additional approximation error, particularly due to the mode truncation. These errors contribute to model-form uncertainty and must be analyzed.

When the HDM depends on parameters, it is often beneficial for the reduced subspace to vary with them, leading to a parameter-to-subspace map  $\mathcal{V}(\boldsymbol{\mu})$ . One can learn such maps from data via interpolation or regression. For example, the Gaussian process subspace (GPS) model places a Gaussian process prior on an extrinsic representation of the basis, inducing a predictive distribution over  $k$ -dimensional subspaces across the parameter domain (Zhang et al., 2022). Allowing  $\mathcal{V}(\boldsymbol{\mu})$  to vary typically improves accuracy over using a fixed  $k$ -dimensional subspace. However, to keep the exposition focused, we restrict attention to a fixed subspace in this paper.

### 2.3 Stochastic reduced-order model

A stochastic reduced-order model (SROM) extends the deterministic ROM by treating the reduced basis as a random quantity. Specifically, instead of the deterministic basis  $\mathbf{V}$ , the SROM uses a stochastic basis  $\mathbf{W}$ . The change from a deterministic basis to a stochastic one introduces randomness into the model and allows it to capture model errors between the ROM, the HDM, and the physical system. The SROM can be written as:

$$\mathbf{x} = \mathbf{W}\mathbf{q}, \quad \dot{\mathbf{q}} = \mathbf{W}^\top \mathbf{f}(\mathbf{W}\mathbf{q}, t; \boldsymbol{\mu}), \quad \mathbf{W} \sim \mu_{\mathbf{V}} \quad (3)$$

where stochastic basis  $\mathbf{W}$  follows a probability distribution  $\mu_{\mathbf{V}}$ . However, it is more natural to impose a probability distribution  $\mu_{\mathcal{V}}$  on the subspace rather than the basis, because the Galerkin projection is uniquely determined by the subspace and is invariant under changes of basis. In this work, we use the stochastic subspace model introduced in Section 3 to sample stochastic basis  $\mathbf{W}$  in a distribution-free and data-driven manner. These stochastic bases form the foundation of SROMs, facilitating the effective characterization of model error.

## 3 Stochastic subspace model

This section develops a bootstrap-based stochastic subspace model. We begin by constructing a deterministic principal subspace via proper orthogonal decomposition (POD), then introduce distribution-free modeling with the bootstrap. Building on these ingredients, we formulate the stochastic subspace model and its associated sampling algorithm. Finally, we present a hyperparameter optimization strategy and outline the key steps for constructing SROMs.

### 3.1 Subspace from the PCA: proper orthogonal decomposition

Principal component analysis (PCA) is widely used for dimension reduction. Closely related to PCA, *proper orthogonal decomposition* (POD) provides a framework for computing the ROM  $\mathbf{V}$  and its associated subspace  $\mathcal{V}$ . Following the notations in Section 2, consider a snapshot matrix  $\mathbf{X} = [\mathbf{x}_1 \cdots \mathbf{x}_m] \in \mathbb{R}^{n \times m}$ , with states  $\mathbf{x}_i = \mathbf{x}(t_i; \boldsymbol{\mu}_i)$ , sample mean  $\bar{\mathbf{x}} = \frac{1}{m} \sum_{i=1}^m \mathbf{x}_i$ , centered snapshot matrix  $\mathbf{X}_0 = \mathbf{X} - \bar{\mathbf{x}}\mathbf{1}_m^\top$ , and sample covariance  $\mathbf{S} = \frac{1}{m} \mathbf{X}_0 \mathbf{X}_0^\top$ . Let  $\mathbf{X}_0 = \mathbf{V}_r \text{diag}(\boldsymbol{\sigma}_r) \mathbf{W}_r^\top$

be a compact singular value decomposition (SVD), where  $\sigma_r \in \mathbb{R}_{>0}^r$  is in non-increasing order. The sample covariance matrix  $\mathbf{S}$  can be written as  $\mathbf{S} = \mathbf{V}_r \text{diag}(\sigma_r/\sqrt{m})^2 \mathbf{V}_r^\top$ . POD selects the *principal basis*  $\mathbf{V}_k$ —the leading  $k$  eigenvectors of  $\mathbf{S}$ —as the deterministic ROB. The corresponding subspace is the *principal subspace*  $\mathcal{V}_k := \text{range}(\mathbf{V}_k)$ . Since all state samples satisfy the linear constraints,  $\mathbf{V}_k$  satisfies the constraints automatically. POD has several other desirable properties: it can extract coherent structures, provide error estimates in  $L^2$  norm, and is computationally efficient and straightforward to implement (Sirovich, 1987).

### 3.2 Bootstrap: distribution-free modeling

The bootstrap (Efron, 1979) is a nonparametric method that approximates the unknown sampling distribution of a statistic by resampling from the empirical distribution of the data. It avoids parametric assumptions about the population distribution and is effective when classical assumptions (e.g., Gaussianity) may be violated.

Given a random sample  $\mathbf{X} = [\mathbf{x}_1 \cdots \mathbf{x}_m]$  drawn from an unknown distribution  $\mathcal{F}$ , the bootstrap method can approximate the sampling distribution of some prespecified random variable  $r(\mathbf{X}; \mathcal{F})$  using the observed data. The bootstrap method constructs the sample probability distribution  $\hat{\mathcal{F}}$  by putting mass  $1/m$  at each observation point  $\mathbf{x}_1, \dots, \mathbf{x}_m$ . Sampling from the empirical distribution  $\hat{\mathcal{F}}$  can be performed by selecting indices randomly:

$$\mathbf{X}^* = [\mathbf{x}_{b_1} \cdots \mathbf{x}_{b_m}], \quad b_i \stackrel{\text{iid}}{\sim} U(\{1, \dots, m\}), \quad i \in \{1, \dots, m\}.$$

Here,  $U(\{1, \dots, m\})$  refers to the uniform distribution over the index set  $\{1, \dots, m\}$ . In simple terms, the bootstrap sample  $\mathbf{X}^*$  is obtained by sampling the observed data with replacement. The bootstrap samples are then used to approximate the sampling distribution of  $r(\mathbf{X}; \mathcal{F})$  by that of  $r^* = r(\mathbf{X}^*; \hat{\mathcal{F}})$ . When the observed data follow a Gaussian distribution, the bootstrap samples can recover the Gaussian behavior. The main advantage of the nonparametric bootstrap emerges when these assumptions are violated: for skewed, heavy-tailed, or multimodal data, resampling from  $\hat{\mathcal{F}}$  propagates the empirical features of the data—such as asymmetry, tail behavior, and multimodality—into the distribution of  $r^*$ . In this way, the bootstrap can reveal uncertainty structures that Gaussian assumptions would obscure, while remaining fully data-driven and free of an explicit parametric model for  $\mathcal{F}$ .

Bootstrap methods have been extended beyond Euclidean settings to respect intrinsic geometric structures. In particular, the normal-bundle bootstrap constructs resamples that preserve a learned data manifold while randomizing along its normal directions (Zhang and Ghanem, 2021). The same geometric perspective applies to our setting: in SROMs the randomized objects are  $k$ -dimensional subspaces, which are points on the Grassmann manifold. Probabilistic models for such subspaces should therefore preserve this manifold structure. Previous works use the matrix angular central Gaussian family, a parametric class of distributions on the Grassmannian, to describe random subspaces (Zhang et al., 2022; Yadav and Zhang, 2025b). Preserving the geometric constraint while increasing modeling flexibility motivates the bootstrap-based stochastic subspace model introduced next.

### 3.3 Stochastic subspace via the bootstrap

We now propose a bootstrap-based stochastic subspace model. Here, the prespecified random variable is the principal subspace, and we approximate its distribution using the resampling approach of the bootstrap method.

Consider the *principal subspace map*  $\pi_k(\mathbf{X}) := \text{range}(\mathbf{U}_k)$ , where  $\mathbf{U}_k$  consists of left singular vectors associated with the  $k$  largest singular values of  $\mathbf{X}$ . As a mapping,  $\pi_k : \mathbb{R}_{k >}^{n \times m} \mapsto \text{Gr}(n, k)$  is uniquely defined for all  $n$ -by- $m$  matrices whose  $k$ -th largest singular value is larger than the  $(k+1)$ -th, with  $k \leq \min(n, m)$ . Using this map, the POD subspace can be written as:

$$\mathcal{V}_k = \pi_k(\mathbf{X}_0). \quad (4)$$

In classical bootstrap methods, each replicate contains the same number of samples as the observed dataset. Here, we introduce a hyperparameter  $\beta$  that decouples the bootstrap sample size from the data size, thereby controlling the effective sample size of the resampled snapshot matrix.

Let  $\mathbf{X}_{0,\beta}^*$  denote a bootstrap-resampled snapshot matrix obtained by sampling the columns of  $\mathbf{X}_0$  randomly with replacement for  $\beta$  times and concatenating them into a matrix. Applying the principal subspace map to  $\mathbf{X}_{0,\beta}^*$  yields a random principal subspace, and repeating this procedure generates a collection of stochastic subspaces. Formally, we define the stochastic subspace model:

$$\mathcal{W} := \pi_k(\mathbf{X}_{0,\beta}^*), \quad (5)$$

where  $\mathbf{X}_{0,\beta}^* \sim \hat{\mathcal{F}}$  is a bootstrap-resampled snapshot matrix with  $\beta \in \{k, k+1, \dots\}$  columns. The close connection of this model with the POD justifies naming it as a *stochastic POD*. The scalar hyperparameter  $\beta$  controls the concentration of the distribution: a larger value corresponds to less variation around  $\mathcal{V}_k$ . Due to its intrinsic POD connection, any stochastic basis  $\mathbf{W}$  sampled from Eq. (5) naturally satisfies linear constraints, i.e.,  $\mathbf{B}^\top \mathbf{W} = 0$ .

A naive implementation of Eq. (5) requires a bootstrap resampling of  $\mathbf{X}_0$  and a truncated SVD, which can be costly when  $n$  is large. However, sampling from this stochastic subspace model can be done very efficiently for  $n \gg 1$  if  $k$  and the rank of  $\mathbf{X}_0$  are small, which is often the case in practical applications. Let  $\mathbf{X}_0 = \mathbf{V}_r \text{diag}(\boldsymbol{\lambda}_r) \mathbf{W}_r^\top$  be a compact SVD where  $r = \text{rank}(\mathbf{X}_0)$ . We can show that:

$$\mathcal{W} = \mathbf{V}_r \pi_k(\text{diag}(\boldsymbol{\lambda}_r) \mathbf{W}_r (\mathbf{b}, :)^{\top}), \quad (6)$$

where  $\mathbf{b} = (b_i)_{i=1}^\beta$  with entries  $b_i \stackrel{\text{iid}}{\sim} U(\{1, \dots, m\})$ . Algorithm 1 describes the corresponding sampling procedure. Using Eq. (6) instead of Eq. (5) reduces the computational cost for truncated SVD from  $O(nk\beta)$  to  $O(rk\beta)$ . Consequently, when applied to the SROM framework, the bootstrap-based stochastic subspace model offers a robust, efficient, and distribution-free mechanism for characterizing and quantifying model-form uncertainty in computational mechanics.

### 3.4 Hyperparameter training

The hyperparameter  $\beta \in \{k, k+1, \dots\}$  is estimated by minimizing the objective function

$$f(\beta) := \mathbb{E}[|d_o(\mathbf{u}_L) - d_o(\mathbf{u}_E)|^2 | \beta], \quad (7)$$

where  $\mathbf{u}_E$  is the experimental or ground-truth observation of the output,  $\mathbf{u}_L$  is the low-fidelity prediction of the SROM, and  $d_o(\mathbf{u}) := \|\mathbf{u} - \mathbf{u}_L^o\|_{L^2}$  is the  $L^2$  distance to the low-fidelity prediction  $\mathbf{u}_L^o$  of a reference model. This objective function aims to improve the consistency of the SROM

---

**Algorithm 1** SS-Bootstrap: Stochastic subspace via Bootstrap.

---

**Input:**  $\mathbf{V}_r$ ;  $\text{diag}(\boldsymbol{\lambda}_r)$ ;  $\mathbf{W}_r$ ; subspace dimension  $k \in \{1, \dots, n\}$ ; resample size  $\beta \in \{k, k+1, \dots\}$ .

- 1: Generate vector  $\mathbf{b} = (b_i)_{i=1}^{\beta}$  with entries  $b_i \stackrel{\text{iid}}{\sim} U(\{1, \dots, m\})$ .
- 2:  $\mathbf{M} \leftarrow \text{diag}(\boldsymbol{\lambda}_r) \mathbf{W}_r (\mathbf{b}, :)^T$ , where  $(\mathbf{b}, :)$  refers to the row selection of matrix  $\mathbf{W}_r$ .
- 3: Truncated SVD:  $[\mathbf{U}_k, \sim, \sim] \leftarrow \text{svd}(\mathbf{M}, k)$ .

**Output:**  $\mathbf{W} = \mathbf{V}_r \mathbf{U}_k$ , an orthonormal basis of a random subspace sampled from the bootstrap model.

---

in characterizing the error of the reference model. We optimize the objective function  $f(\beta)$  efficiently using our Bayesian optimization under uncertainty framework tailored to concentration-parameter training in stochastic models (Yadav and Zhang, 2025a). The Bayesian optimization under uncertainty framework utilizes a statistical surrogate for the underlying random variable, allowing for the analytical evaluation of the expectation operator. Moreover, it provides a closed-form expression for the optimizer of the random acquisition function, which significantly reduces the computational cost per iteration compared to optimization approaches based on Monte Carlo approximation of the expectation.

### 3.5 Construction of SROM using SS-Bootstrap

The main steps of the proposed approach to stochastic reduced-order modeling are listed below:

1. **Solve HDM and collect snapshots:** Run the HDM and store state vectors at selected times and/or parameters to form the snapshot matrix  $\mathbf{X} = [\mathbf{x}_1, \dots, \mathbf{x}_m]$ .
2. **Extract deterministic ROB:** Center the snapshots  $\mathbf{X}_0 = \mathbf{X} - \bar{\mathbf{x}}\mathbf{1}_m^T$ , where  $\bar{\mathbf{x}} = \frac{1}{m} \sum_{i=1}^m \mathbf{x}_i$ . Perform a compact SVD:  $\mathbf{X}_0 = \mathbf{V}_r \text{diag}(\boldsymbol{\sigma}_r) \mathbf{W}_r^T$ . Select  $k$  as the smallest integer  $j$  satisfying  $\sum_{i=1}^j \sigma_i^2 \geq \tau \sum_{i=1}^r \sigma_i^2$ , where  $\tau \in (0, 1)$  is a prescribed variance threshold. Set the deterministic ROB to the first  $k$  singular vectors  $\mathbf{V}_k$ .
3. **Solve ROM:** Substitute  $\mathbf{V}_k$  into Eq. (2) to obtain the deterministic ROM solution.
4. **Tune stochastic subspace model:** Using SS-Bootstrap Algorithm 1, generate stochastic subspaces  $\mathcal{W}$  with bases  $\mathbf{W} = \mathbf{V}_r \mathbf{U}_k$ , and tune the concentration parameter  $\beta \in [k, \infty)$  according to the criterion in Eq. (7).
5. **Build SROM ensemble:** With the tuned  $\beta$ , sample  $\mathcal{W}$  to produce stochastic bases  $\mathbf{W}$  to replace  $\mathbf{V}_k$  in Eq. (2). The resulting ensemble of SROM realizations quantifies the model and truncation errors through the variability of their outputs.

These steps are applicable to both linear and nonlinear systems. For linear systems, however, the cost of SROM construction can be reduced substantially. Naively, each SROM realization requires constructing a stochastic basis  $\mathbf{W} = \mathbf{V}_r \mathbf{U}_k$  and projecting the HDM onto this basis. This cost accumulates with the number of SROM samples. A more efficient strategy is to perform a two-stage reduction: first project the operators once onto the rank- $r$  subspace spanned by  $\mathbf{V}_r$  (e.g.,  $\mathbf{A}_r = \mathbf{V}_r^T \mathbf{A} \mathbf{V}_r$  for any system matrix  $\mathbf{A}$ ); and then for each stochastic basis  $\mathbf{U}_k$  sampled in this  $r$ -dimensional subspace, compute  $\mathbf{A}_w = \mathbf{U}_k^T \mathbf{A}_r \mathbf{U}_k$  so that the overall basis is  $\mathbf{W} = \mathbf{V}_r \mathbf{U}_k$ . This two-stage reduction avoids repeated high-dimensional operator projections and significantly lowers the SROM construction cost.

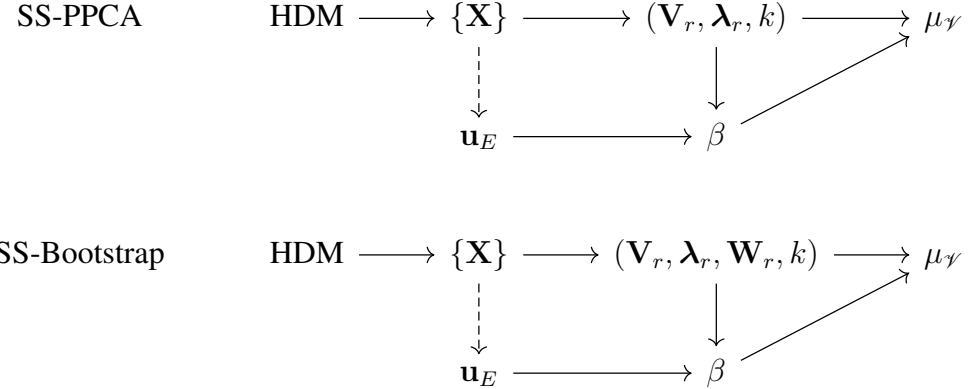


Figure 1: Dependence diagrams for (from top to bottom) the SS-PPCA and the SS-Bootstrap models of stochastic subspace. The dashed lines indicate that the connection only exists when characterizing the ROM-to-HDM error.

## 4 Related work

While NPM and RSM also fall within the SROM framework, both methods model the reduced-order basis, which makes them less suitable for direct comparison with the proposed approach. Consequently, this section reviews SS-PPCA, compares its operational mechanics with those of SS-Bootstrap, and presents evaluation metrics for stochastic models.

### 4.1 Stochastic subspace via probabilistic principal component analysis (SS-PPCA)

Given  $\mathbf{X} = [\mathbf{x}_1 \cdots \mathbf{x}_m] \in \mathbb{R}^{n \times m}$  a sample of the state, with  $\mathbf{x}_i = \mathbf{x}(t_i; \boldsymbol{\mu}_i)$ , sample mean  $\bar{\mathbf{x}} = \frac{1}{m} \sum_{i=1}^m \mathbf{x}_i$ , centered sample  $\mathbf{X}_0 = \mathbf{X} - \bar{\mathbf{x}}\mathbf{1}_m^\top$ , and sample covariance  $\mathbf{S} = \frac{1}{m} \mathbf{X}_0 \mathbf{X}_0^\top$ , SS-PPCA (Yadav and Zhang, 2025b) models the unknown data distribution as  $\tilde{\mathbf{x}} \sim N_n(\bar{\mathbf{x}}, \mathbf{S})$ . The stochastic subspace via SS-PPCA is then defined as:

$$\mathcal{W} := \pi_k(\tilde{\mathbf{X}}_{0,\beta}) \stackrel{\text{def}}{\sim} \text{MACG}_{n,k,\beta}(\mathbf{S}), \quad (8)$$

where  $\tilde{\mathbf{X}}_{0,\beta} \sim N_{n,\beta}(0; \mathbf{S}, \mathbf{I}_\beta)$  is a  $\beta$ -sample matrix and  $\beta \in \{k, k+1, \dots\}$  is the resample size.

Intuitively, SS-PPCA first postulates a multivariate Gaussian model for the snapshots with mean  $\bar{\mathbf{x}}$  and covariance  $\mathbf{S}$ , then draws a random snapshot matrix from this distribution to obtain  $\tilde{\mathbf{X}}_{0,\beta}$ . Applying the map  $\pi_k(\cdot)$  extracts the leading  $k$ -dimensional principal subspace, inducing a matrix angular central Gaussian (MACG) distribution over  $k$ -dimensional subspaces. This distribution can be sampled efficiently using a low-rank decomposition of  $\mathbf{S}$ . Let  $\mathbf{S} = \mathbf{V}_r \text{diag}(\boldsymbol{\lambda}_r) \mathbf{V}_r^\top$  be a compact EVD, where  $r = \text{rank}(\mathbf{S})$ . The stochastic subspace can be written as:

$$\mathcal{W} = \mathbf{V}_r \pi_k \left( \text{diag}(\boldsymbol{\lambda}_r)^{1/2} \mathbf{Z}_{r \times \beta} \right), \quad (9)$$

where  $\mathbf{Z}_{r \times \beta}$  is an  $r$ -by- $\beta$  standard Gaussian matrix. This low-rank form allows SS-PPCA sampling to be performed in  $O(rk\beta)$  flops, the same computational complexity as SS-Bootstrap.

However, because SS-PPCA is built on a Gaussian latent variable model, the resulting stochastic subspaces may struggle to capture non-Gaussian structure in the underlying data, such as skewness, heavy tails, or multimodality, potentially impacting its performance in such cases.

## 4.2 Comparison of model structures

To deepen understanding of the two methods, we outline their structures in Fig. 1 and highlight the key differences below. Both SS-PPCA and SS-Bootstrap (i) model principal subspaces, (ii) do not require discretization information, (iii) use a single scalar hyperparameter, and (iv) allow quantities of interest in the objective in training the hyperparameter. Their primary distinction lies in modeling assumptions: SS-PPCA posits a Gaussian latent-variable model on the system state and derives distributions for random matrices and their principal subspaces, whereas SS-Bootstrap draws directly from the empirical data distribution via resampling to induce a distribution over principal subspaces. The nonparametric nature of SS-Bootstrap allows it to adapt to the data distribution, providing robustness to distributional misspecification. By generating data-consistent stochastic subspaces, SS-Bootstrap leads to SROMs that perturb the reference physics only along directions supported by the data, allowing for sharper and more reliable characterization of model error.

## 4.3 Metrics for comparing stochastic models

We evaluate the two stochastic subspace models using two general metrics: consistency and sharpness. By *consistent* UQ, we mean that the statistics on prediction uncertainty—such as standard deviation and predictive intervals (PI)—derived from the model match the prediction error on average. Without consistency, the model either under- or over-estimates its prediction error, which risks being over-confident or unnecessarily conservative. By *sharp* UQ, we mean the model’s PIs are narrower than alternative methods. This is essentially the probabilistic version of model accuracy and is desirable as we want to minimize error.

## 5 Numerical examples

This section compares the proposed method, SS-Bootstrap, with SS-PPCA in characterizing model error using two numerical examples. First, we consider a parametric linear static problem with non-Gaussian data. Second, we examine a linear dynamics problem involving a space structure. All data and code are available at [https://github.com/UQUH/SS\\_Bootstrap](https://github.com/UQUH/SS_Bootstrap).

### 5.1 Parametric linear static problem

We consider a one-dimensional parametric linear static problem with  $n = 1000$  degrees of freedom (DoFs), governed by

$$\mathbf{K}\mathbf{x}(\boldsymbol{\mu}) = \mathbf{f}(\boldsymbol{\mu}), \quad (10)$$

where  $\mathbf{x}(\boldsymbol{\mu}) \in \mathbb{R}^n$  is the displacement vector, and  $\boldsymbol{\mu} \in [0, 1]^2$  is a parameter vector which controls the loading conditions. Homogeneous Dirichlet boundary conditions are imposed at the first and last nodes,  $x_1(\boldsymbol{\mu}) = x_n(\boldsymbol{\mu}) = 0$ , which can be expressed compactly as  $\mathbf{B}^\top \mathbf{x}(\boldsymbol{\mu}) = 0$  with  $\mathbf{B} = [\mathbf{e}_1, \mathbf{e}_n]$ , where  $\mathbf{e}_i$  denotes the  $i$ -th standard basis vector. The stiffness matrix  $\mathbf{K} \in \mathbb{R}^{n \times n}$  is constructed as  $\mathbf{K} = \boldsymbol{\Phi} \boldsymbol{\Lambda} \boldsymbol{\Phi}^\top$ , with  $\boldsymbol{\Lambda} = \text{diag}(4\pi^2 j^2)_{j=1}^{n-2}$  and  $\boldsymbol{\Phi} = [0 \ \mathbf{S} \ 0]^\top$ . The matrix  $\mathbf{S} = \sqrt{\frac{2}{n-1}} [\sin(\frac{jk\pi}{n-1})]_{k=1, \dots, n-2}^{j=1, \dots, n-2}$  is the order- $(n-2)$  type-I discrete sine transform (DST-I) matrix, scaled to be orthogonal. Thus,  $\mathbf{K}$  has eigenpairs  $(\lambda_j, \boldsymbol{\phi}_j)$  with  $\lambda_j = 4\pi^2 j^2$  and  $\boldsymbol{\phi}_j$  is the  $j$ th column of  $\boldsymbol{\Phi}$ . The loading is parameterized as

$$\mathbf{f}(\boldsymbol{\mu}) = \frac{\mathbf{g}(\boldsymbol{\mu})}{\|\mathbf{g}(\boldsymbol{\mu})\|_\infty}, \quad \mathbf{g}(\boldsymbol{\mu}) = \mu_1(\boldsymbol{\phi}_2 + \boldsymbol{\phi}_3) + \mu_2(\boldsymbol{\phi}_4 + \boldsymbol{\phi}_5), \quad (11)$$

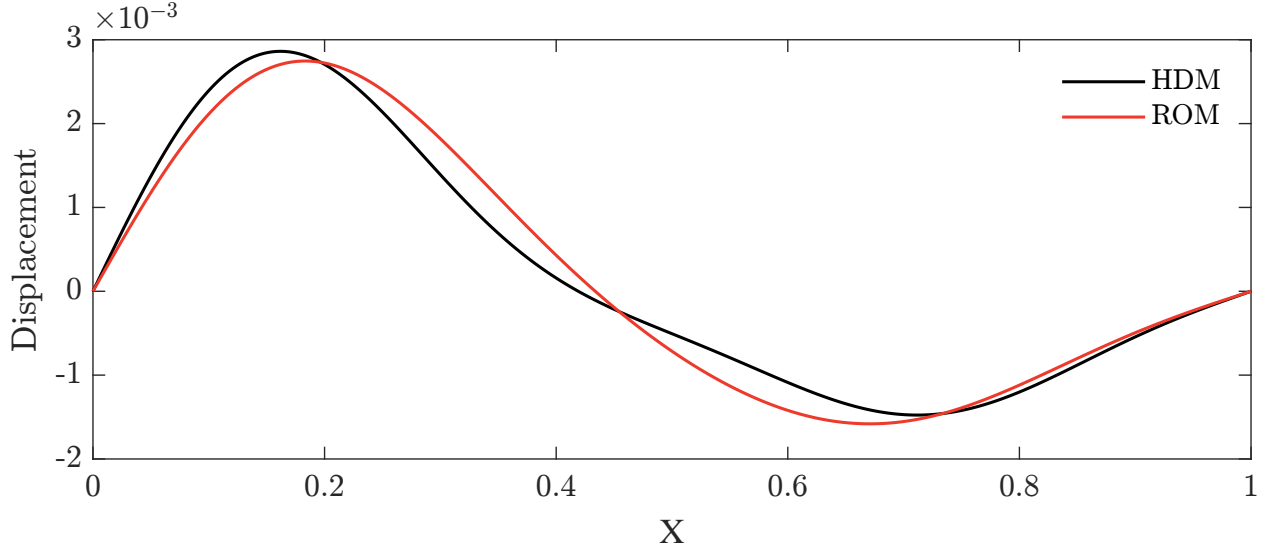


Figure 2: HDM vs ROM displacement at the test parameter

with  $\mu_1, \mu_2 \sim \beta(0.5, 0.5)$ , i.e., the force depends upon the parameters  $\mu_i$ . This setup provides a controlled framework for studying parameter-dependent structural responses, especially in the context of model error.

Since  $\mathbf{K}$  is independent of  $\mu$ , it can be factorized once and stored for efficient inversion, but more general parametric HDMs are significantly more expensive to evaluate—justifying ROM construction. We construct a ROM by sampling 50 parameter points from the  $\beta$ -distribution,  $\mu_1, \mu_2 \sim \beta(0.5, 0.5)$ . For each sample, we solve  $\mathbf{x}_j = \mathbf{K}^{-1}\mathbf{f}(\mu_j)$ ,  $j = 1, \dots, 50$ , and form the snapshot matrix  $\mathbf{X} = [\mathbf{x}_1, \dots, \mathbf{x}_{50}]$ . The deterministic ROB  $\mathbf{V} = \pi_k(\mathbf{X})$  with dimension  $k = 1$  is obtained via POD. The governing equation of the ROM is given by:

$$\mathbf{x}_R = \mathbf{V}\mathbf{q}, \quad \mathbf{K}_k\mathbf{q} = \mathbf{V}^\top\mathbf{f}(\mu), \quad \mathbf{K}_k = \mathbf{V}^\top\mathbf{K}\mathbf{V}. \quad (12)$$

To evaluate ROM accuracy, we define a test parameter  $\mu_{\text{test}} = [\frac{1}{2}, \frac{1}{2}]$ , which lies within the parameter domain but is not included in the training set. Figure 2 compares the HDM and ROM displacement at the test parameter.

To characterize ROM-induced error, we construct SROMs by replacing the deterministic ROB  $\mathbf{V}$  with SROBs  $\mathbf{W}$ . For SS-Bootstrap, SROBs  $\mathbf{W}$  are sampled using the stochastic subspace model described in Section 3.3 and Algorithm 1. For SS-PPCA, SROBs  $\mathbf{W}$  are sampled using the stochastic subspace model described in (Yadav and Zhang, 2025b). In both cases, the hyperparameter  $\beta$  is optimized by minimizing the objective function in Eq. (7), where  $\mathbf{u}_E$  denotes HDM displacements at the training parameters and  $\mathbf{u}_L^o$  denotes the corresponding ROM displacements. For this example, the optimal  $\beta$  via SS-Bootstrap is 8, and training requires 1.3 seconds.

Figures 3 and 4 compare SROM predictions from SS-Bootstrap and SS-PPCA for the linear static example. For both methods, the 95% prediction interval (PI) is estimated using 1000 Monte Carlo samples of the SROM, ensuring a consistent basis for comparison. The empirical coverage—95.6% for SS-Bootstrap and 96.9% for SS-PPCA—indicates that both approaches produce uncertainty bounds that are statistically consistent with the underlying HDM response. However, the average PI width for SS-PPCA is  $1.9 \times$  that of SS-Bootstrap, highlighting the sharper uncertainty quantification provided by the proposed method. This behavior reflects the underlying assumptions of the two

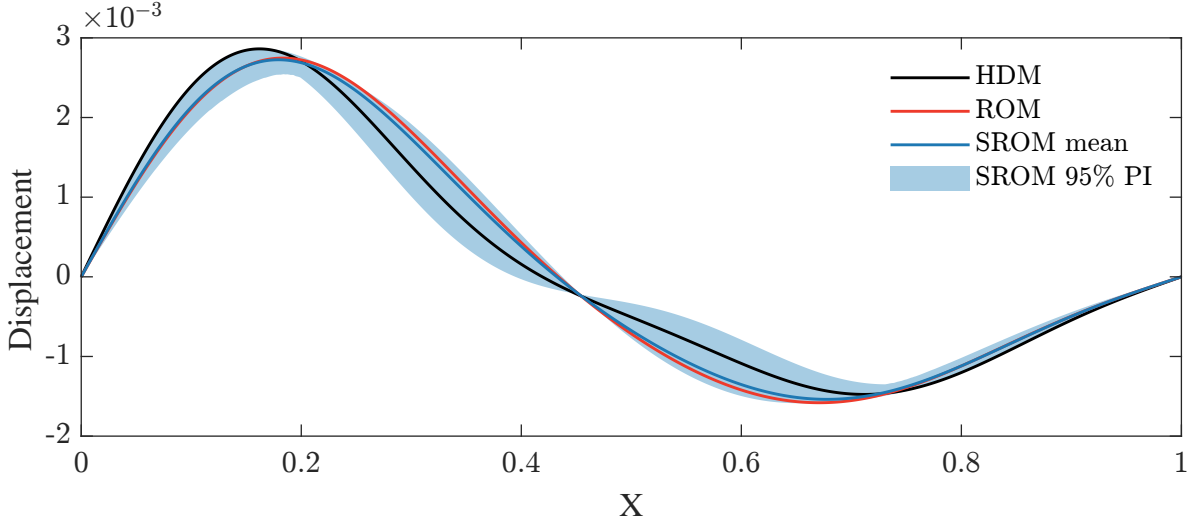


Figure 3: Linear Static Problem: prediction using Bootstrap.

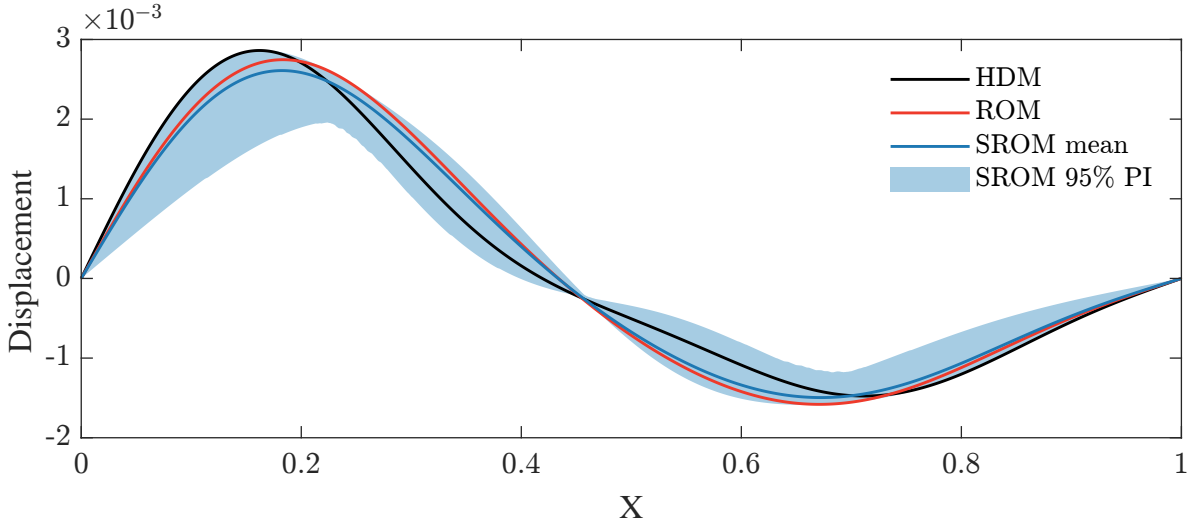


Figure 4: Linear Static Problem: prediction using PPCA.

methods. SS-PPCA relies on a Gaussian latent-variable model, which can induce conservative subspace variability when the snapshot distribution is non-Gaussian, as is the case here due to the Beta-distributed loading parameters. In contrast, SS-Bootstrap constructs stochastic subspaces directly from the empirical snapshot distribution, leading to subspace variability that is better aligned with the observed data and, consequently, to sharper PIs with comparable coverage.

## 5.2 Linear dynamics: space structure

We consider a major component of a space structure (Zeng and Ghanem, 2023), see Fig. 5a. The space structure comprises two parts: an open upper section and a lower section. A large mass (approximately 100 times heavier than the remainder of the model) is located at the center of the upper section and is connected to the sidewalls via rigid links. The lower section consists of an outer cylindrical shell and an inner shock absorption block with a hollow cavity that houses essential components. The impulse load (Fig. 5b) is applied at the mass center along the  $z$ -direction,

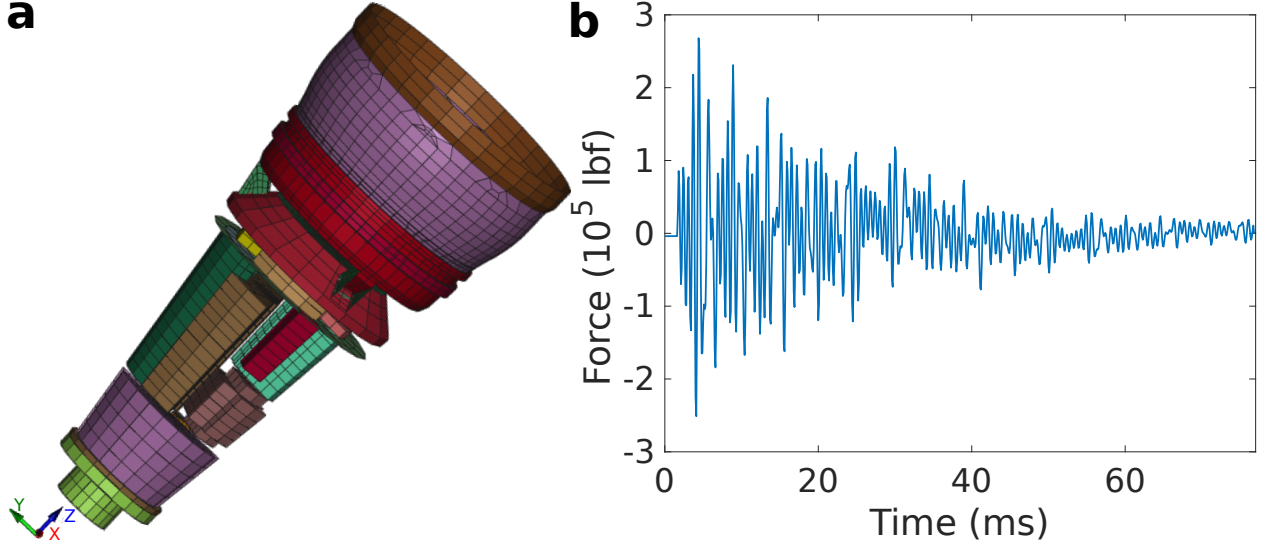


Figure 5: Linear Dynamics: space structure.

transmitted to the upper section through the sidewalls, and then to the lower section via the mounting pedestal. Because the load can compromise the functionality of essential components, we monitor acceleration and velocity at critical points to ensure safe operation. The quantity of interest (QoI) is the  $x$ -velocity at a critical point on one essential component. The space structure has no boundary conditions; it can be assumed to be floating in space. The governing equation of the HDM of the space structure is given by:

$$\mathbf{M}_H \ddot{\mathbf{x}} + \mathbf{C}_H \dot{\mathbf{x}} + \mathbf{K}_H \mathbf{x} = \mathbf{f}, \quad (13)$$

with initial conditions  $\mathbf{x}(0) = \mathbf{0}$  and  $\dot{\mathbf{x}}(0) = \mathbf{0}$ . The matrices  $\mathbf{M}_H$ ,  $\mathbf{K}_H$ , and the force vector  $\mathbf{f}$  are exported from an LS-DYNA finite element model; the damping is Rayleigh,  $\mathbf{C}_H = \beta_H \mathbf{K}_H$ , with  $\beta_H = 6.366 \times 10^{-6}$ . The HDM response  $\mathbf{x}_H$  is computed via the Newmark- $\beta$  method with a time step of  $5 \times 10^{-2}$  ms. One HDM run takes approximately 38 minutes, which is prohibitive for repeated evaluations. To reduce cost, we construct a POD-based ROM of dimension  $k = 10$ . The ROM derived from the HDM is defined as

$$\mathbf{x}_R = \mathbf{V}\mathbf{q}, \quad \mathbf{M}_{H,V} \ddot{\mathbf{q}} + \mathbf{C}_{H,V} \dot{\mathbf{q}} + \mathbf{K}_{H,V} \mathbf{q} = \mathbf{V}^\top \mathbf{f}, \quad (14)$$

where reduced matrices are denoted with a pattern  $\mathbf{A}_V := \mathbf{V}^\top \mathbf{A} \mathbf{V}$ , so that  $\mathbf{M}_{H,V} = \mathbf{V}^\top \mathbf{M}_H \mathbf{V}$ , for example. The initial condition of ROM is given by  $\mathbf{q}(0) = \mathbf{0}$  and  $\dot{\mathbf{q}}(0) = \mathbf{0}$ . The ROM runs in 0.2 seconds—about  $1.12 \times 10^4$  times faster than the HDM—at the expense of approximation error. We therefore use SROMs for error characterization by replacing the deterministic ROB  $\mathbf{V}$  with stochastic ROBs (SROBs)  $\mathbf{W}$ .

For SS-Bootstrap,  $\mathbf{W}$  is sampled using the stochastic subspace model defined in [Section 3.3](#) and [Algorithm 1](#). For SS-PPCA,  $\mathbf{W}$  is sampled using the probabilistic PCA-based model described in ([Yadav and Zhang, 2025b](#)). Here,  $\mathbf{u}_E$  is the HDM velocity at the critical node and  $\mathbf{u}_L^o$  is the ROM velocity at the same location. The optimal hyperparameter via the bootstrap method is  $\beta = 69$ , obtained using the procedure in [Section 3.4](#). Training takes 19.4 seconds, which is negligible relative to an HDM run, indicating good scalability.

[Figures 6](#) and [7](#) compare the velocity prediction of SS-Bootstrap and SS-PPCA. Although the two methods yield visually similar envelopes, SS-Bootstrap consistently produces sharper PIs (see

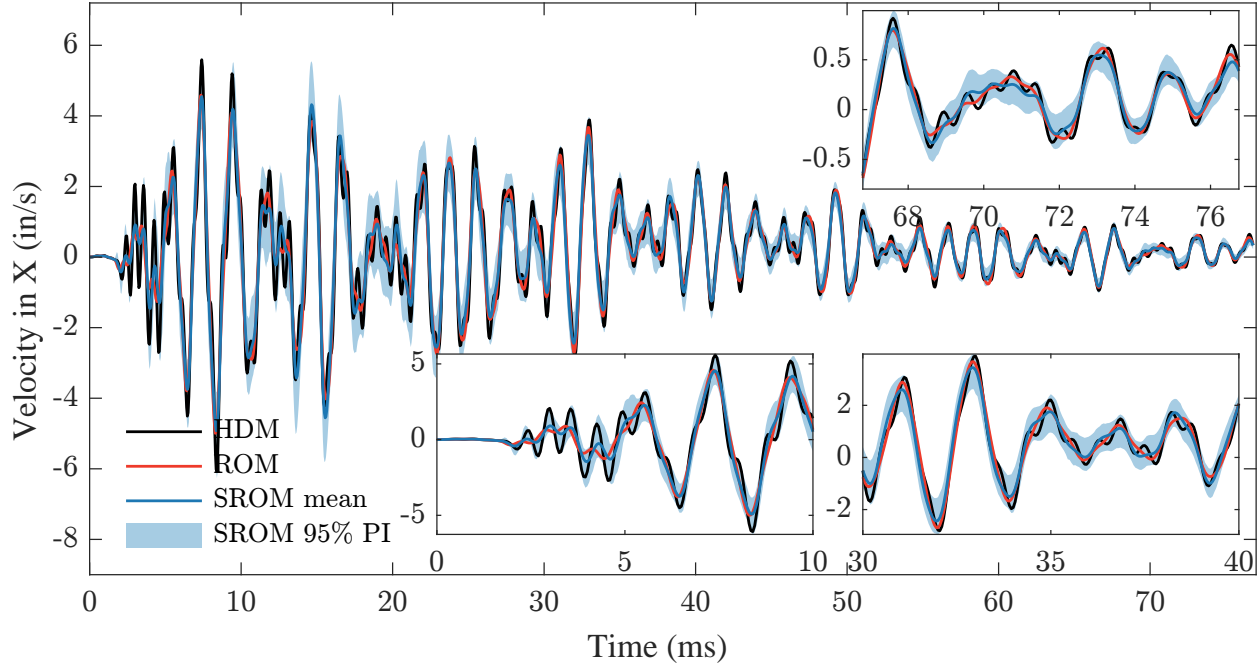


Figure 6: Dynamic prediction of the Bootstrap model: velocity.

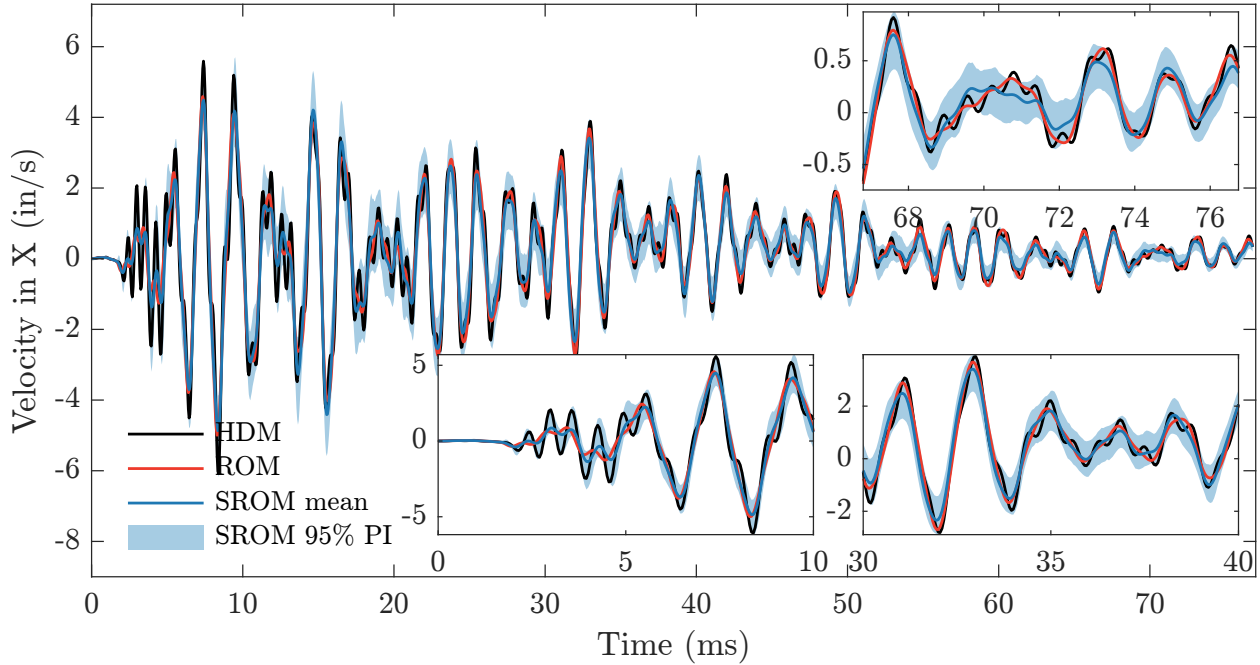


Figure 7: Dynamic prediction of the PPCA model: velocity.

**Table 1**). The HDM velocity exhibits high-frequency behavior during the initial 0–10 ms, which ROM cannot fully capture. Both stochastic models characterize this error well, with SS-PPCA achieving reasonable coverage (93.34%) but with wider PIs, whereas SS-Bootstrap attains higher coverage (95.58%) along with tighter bounds.

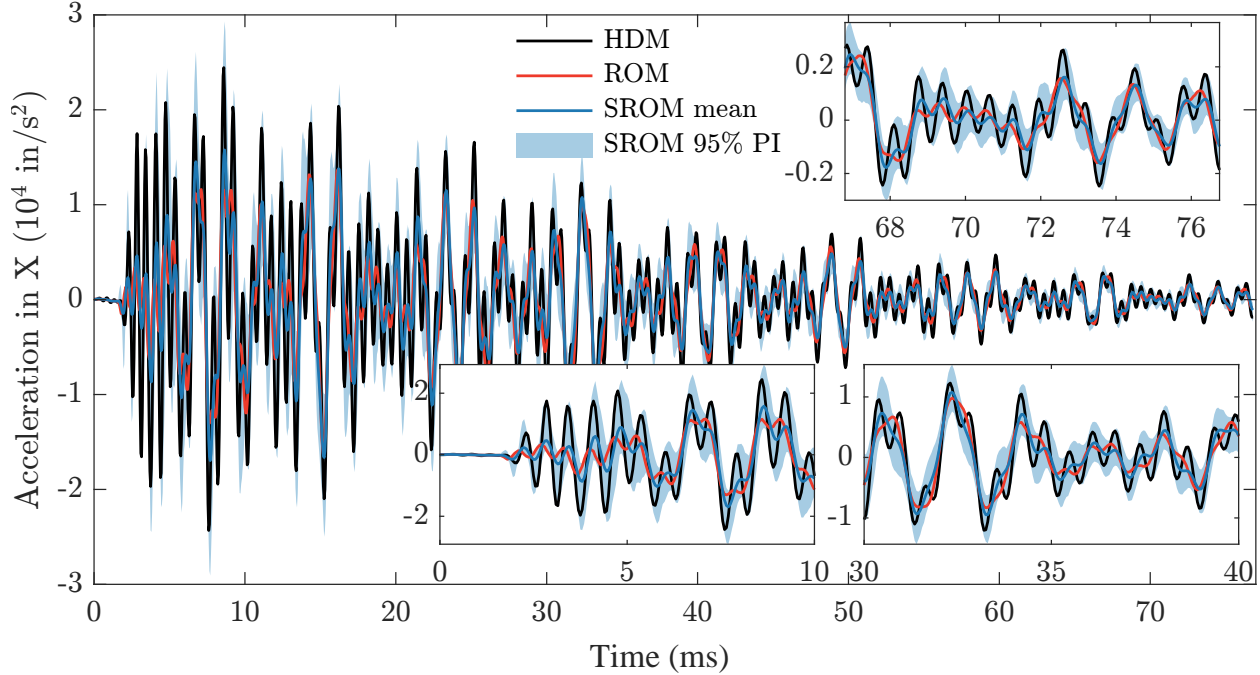


Figure 8: Dynamic prediction of the Bootstrap model: acceleration.

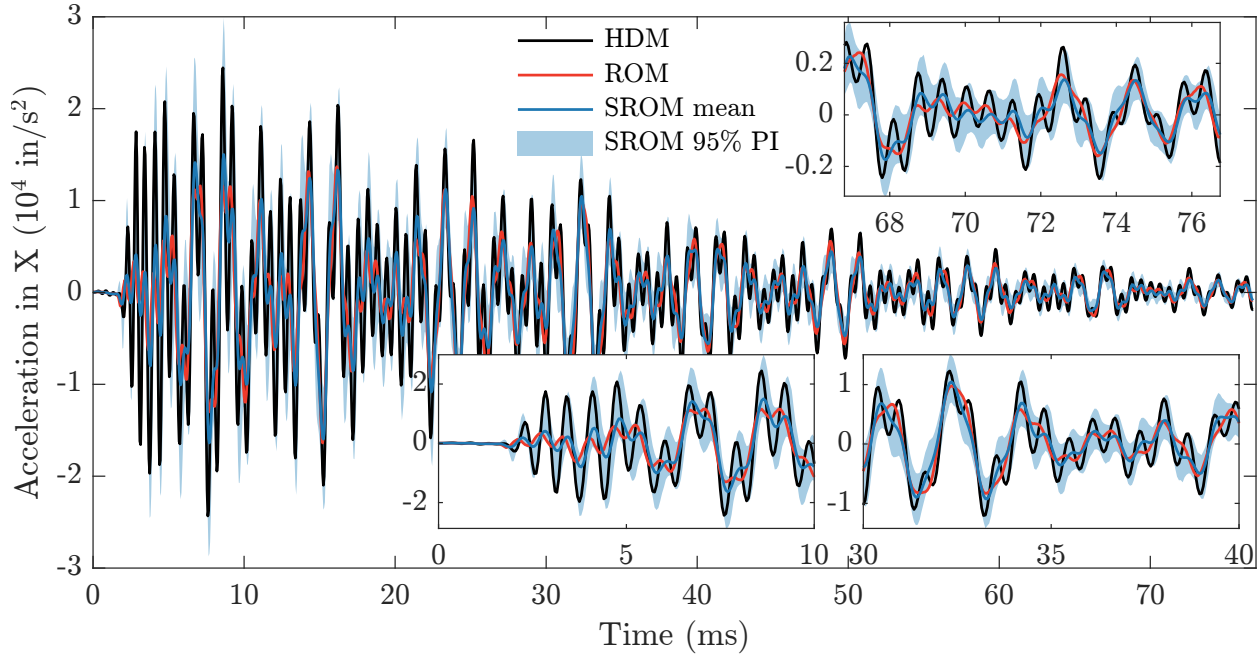


Figure 9: Dynamic prediction of the PPCA model: acceleration.

A similar trend appears for acceleration predictions (Figs. 8 and 9). Both methods track the overall HDM response, but SS-Bootstrap again yields narrower PIs while maintaining higher coverage (87.06% vs. 84.14%). This indicates that the bootstrap-based approach captures the high-frequency variability introduced by the impulse more effectively than SS-PPCA, benefiting from its direct use of the empirical snapshot distribution rather than a Gaussian latent-variable model.

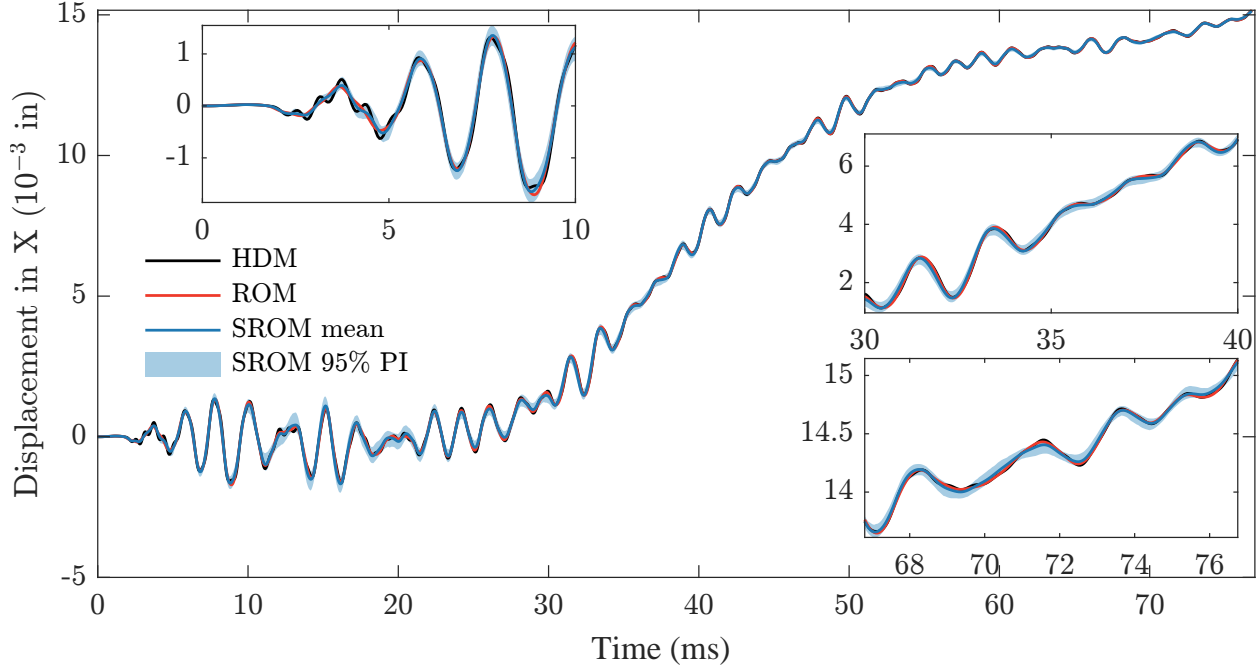


Figure 10: Dynamic prediction of the Bootstrap model: displacement.

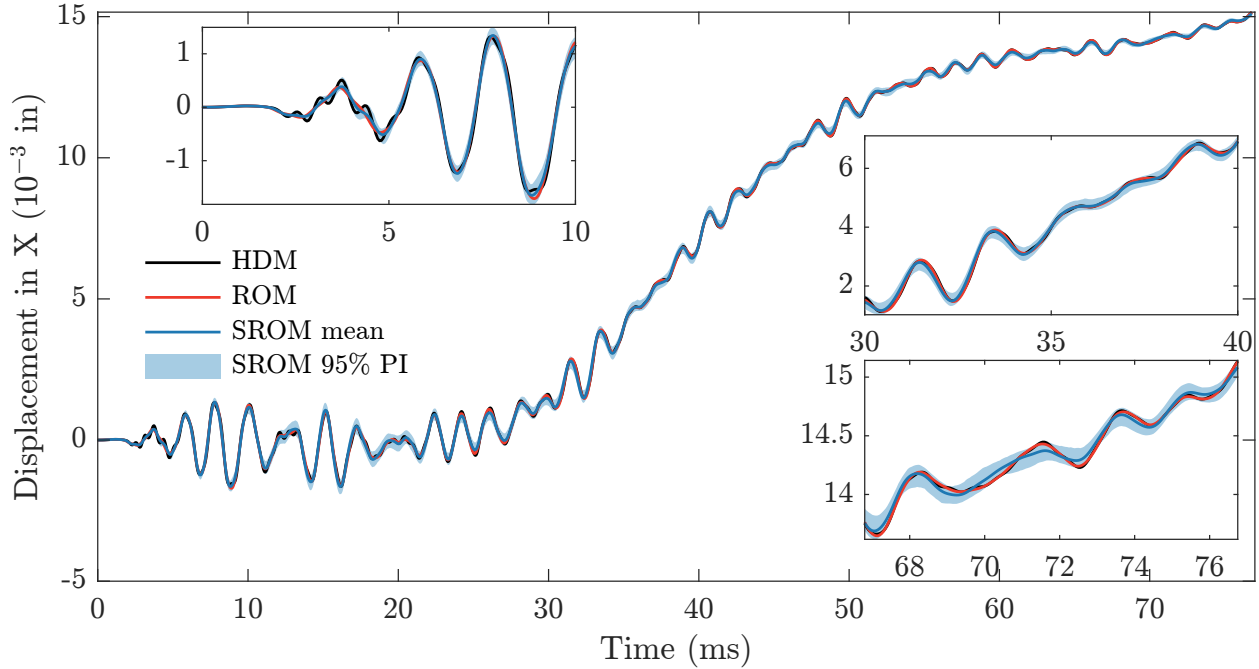


Figure 11: Dynamic prediction of the PPCA model: displacement.

It is important to note that, although the hyperparameter is trained using velocity (the QoI in this example) and the deterministic ROB V is obtained from displacement snapshots, the approach enables predictions for unobserved quantities such as acceleration. More broadly, it supports the efficient prediction of unobserved QoIs across the system—a capability often lacking in related studies—thereby enhancing its practical applicability.

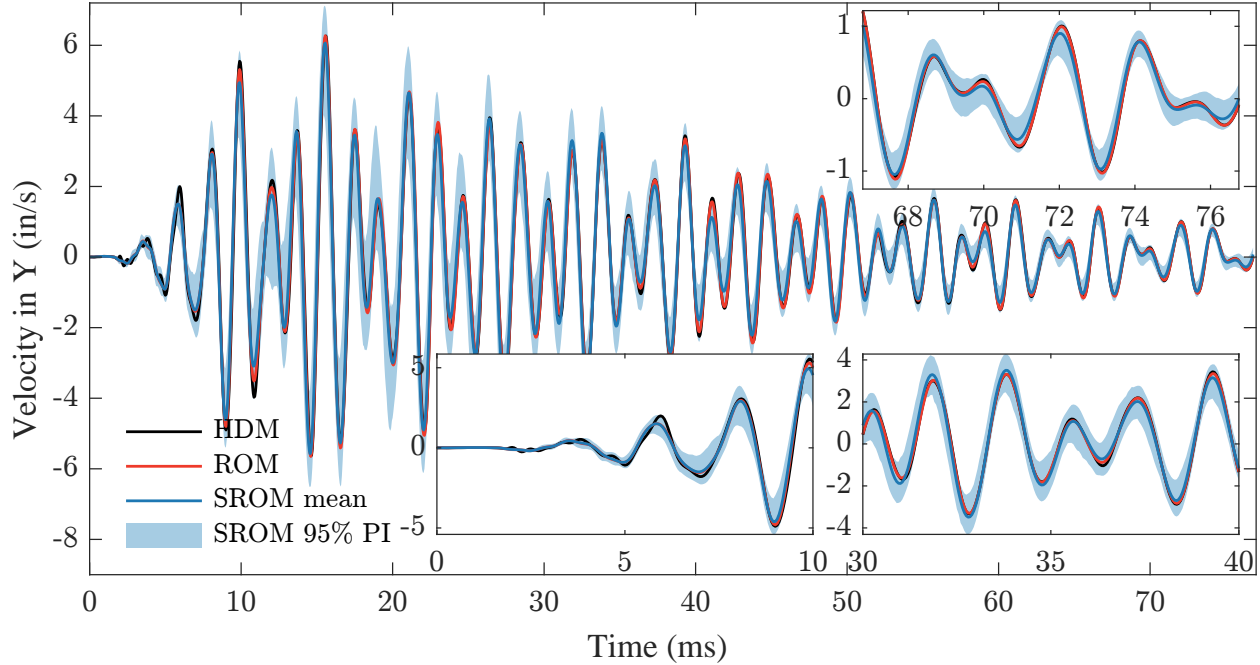


Figure 12: Dynamic prediction of the Bootstrap model: velocity at a random dof.

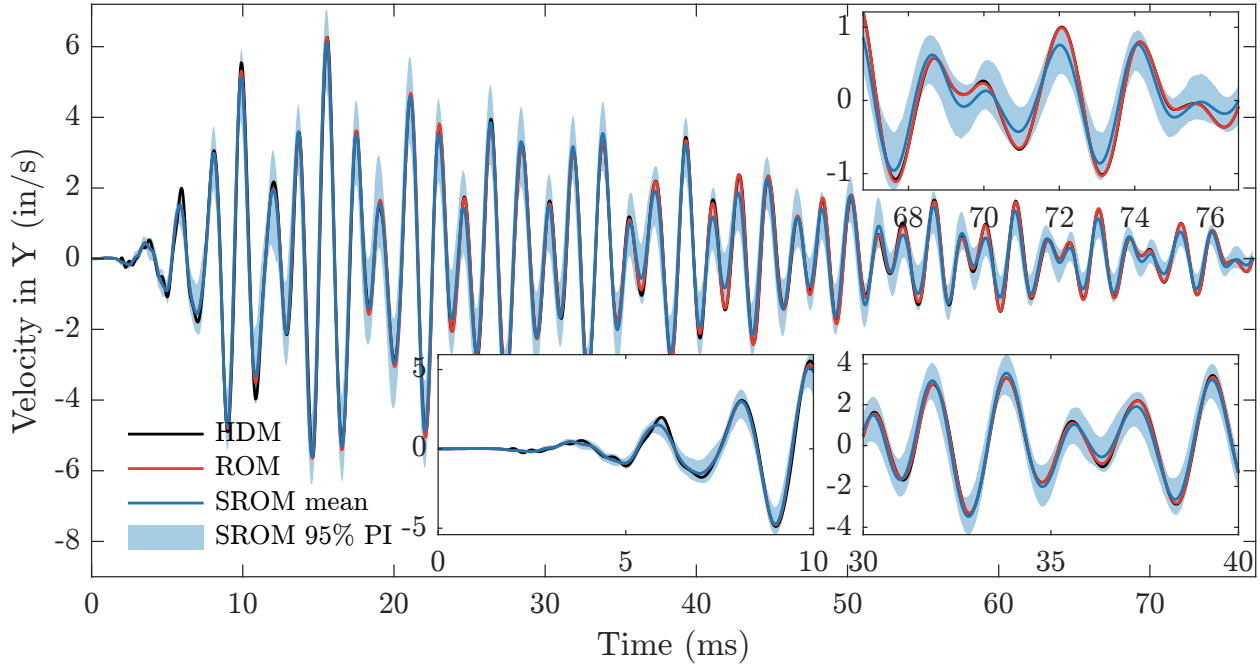


Figure 13: Dynamic prediction of the SS-PPCA model: velocity at a random dof.

Figures 10 and 11 reports the displacement predictions at the same node. SS-PPCA provides accurate and consistent estimates (96.11% coverage), yet SS-Bootstrap achieves comparable or better coverage (97.08%) with substantially narrower PIs (see Table 1), demonstrating improved sharpness across QoIs.

Table 1: Dynamics problem: consistency and sharpness of 95% PI.

95% PI	SS-PPCA		SS-Bootstrap		width ratio <sup>‡</sup>
	coverage <sup>*</sup>	width <sup>†</sup>	coverage <sup>*</sup>	width <sup>†</sup>	
$d_x$ ( $10^{-4}$ in)	<u>96.11%</u>	3.17	<b>97.08%</b>	<b>2.69</b>	<b>1.37</b>
$v_x$ (in/s)	93.34%	1.18	<u>95.58%</u>	<b>1.11</b>	<b>1.19</b>
$a_x$ ( $10^3$ in/s <sup>2</sup> )	84.14%	<b>7.26</b>	<u>87.06%</u>	7.22	<b>1.04</b>
$v_r$ (in/s)	<u>93.42%</u>	<b>1.41</b>	<b>96.63%</b>	1.51	<b>1.11</b>

<sup>\*</sup> Proportion of true response covered by the 95% PI: larger numbers are in boldface; numbers closer to 95% are in underline.

<sup>†</sup> Average width of 95% PIs: smaller numbers are in boldface.

<sup>‡</sup> Average ratio of 95% PI widths, PPCA vs. Bootstrap: numbers larger than one are in boldface.

While the results above focus on a single critical node, many applications require predictions at other locations or system-level behavior. Both SROM approaches generalize to unobserved DOFs, as shown in [Figs. 12](#) and [13](#). The SROM mean under SS-Bootstrap remains closer to both the HDM and deterministic ROM predictions, whereas SS-PPCA exhibits slightly larger deviations. Nonetheless, both methods maintain consistency, with SS-Bootstrap providing uniformly narrower PIs and thus more efficient uncertainty quantification for system-level predictions.

SS-PPCA and SS-Bootstrap provide automated and efficient training with a single hyperparameter. While SROM-based methods cannot fully eliminate model error (since they are built on a ROM), accuracy can be improved by increasing the number of reduced bases or adding closure terms; see [Ahmed et al. \(2021\)](#) for a review on ROM closure.

## 6 Conclusion

We introduced a bootstrap-based stochastic subspace model for characterizing model error within the framework of stochastic reduced-order models. The proposed SS-Bootstrap method is simple, efficient, and straightforward to implement. It requires only one hyperparameter, which is optimized systematically to ensure consistency.

Through numerical examples, we demonstrated that SS-Bootstrap provides sharper and more reliable uncertainty quantification than the existing SS-PPCA approach. The method consistently captured different sources of model error, including parametric uncertainty and ROM truncation error, while maintaining a low computational cost.

While the bootstrap procedure presented in this paper applies to constructing randomized principal subspaces of data matrices and is applied to POD-based reduced-order models, the same procedure may also be applied to other sampling-based model reduction approaches, such as the reduced basis method and dynamic mode decomposition. Moreover, the framework integrates naturally with methods for propagating aleatory uncertainty. Each random realization of the aleatory inputs can be propagated through a random realization of the SROM, yielding an ensemble that captures the combined effects of all uncertainties in a consistent and computationally tractable way.

Although the test cases focused on linear systems, the approach is generally applicable to nonlinear problems as well. In regimes with very large errors, however, characterization alone may be insufficient. Future work will therefore investigate practical strategies for model error correction, building on the robust characterization enabled by SS-Bootstrap.

## 7 Acknowledgments

This work was funded by the University of Houston through the SEED program no. 000189862.

## References

Ahmed, S. E., Pawar, S., San, O., Rasheed, A., Iliescu, T., and Noack, B. R. (2021). “On closures for reduced order models—a spectrum of first-principle to machine-learned avenues.” *Physics of Fluids*, 33(9), 091301.

Arendt, P., Apley, D., and Chen, W. (2012). “Quantification of model uncertainty: Calibration, model discrepancy, and identifiability.” *Journal of Mechanical Design*, 134, 100908.

Azzi, M.-J., Ghnatis, C., Avery, P., and Farhat, C. (2022). “Acceleration of a physics-based machine learning approach for modeling and quantifying model-form uncertainties and performing model updating.” *Journal of Computing and Information Science in Engineering*, 23(1).

Brynjarsdóttir, J. and O’Hagan, A. (2014). “Learning about physical parameters: the importance of model discrepancy.” *Inverse Problems*, 30(11), 114007.

Chopra, A. K. (1996). “Modal analysis of linear dynamic systems: Physical interpretation.” *Journal of Structural Engineering*, 122(5), 517–527.

Efron, B. (1979). “Bootstrap methods: Another look at the jackknife.” *The Annals of Statistics*, 7(1), 1–26.

Efron, B. and Tibshirani, R. (1994). *An Introduction to the Bootstrap*. Chapman and Hall/CRC (May).

Girolami, M., Febrianto, E., Yin, G., and Cirak, F. (2021). “The statistical finite element method (statfem) for coherent synthesis of observation data and model predictions.” *Computer Methods in Applied Mechanics and Engineering*, 375, 113533.

Higdon, D., Gattiker, J., Williams, B., and Rightley, M. (2008). “Computer model calibration using high-dimensional output.” *Journal of the American Statistical Association*, 103(482), 570–583.

Higdon, D., Kennedy, M., Cavendish, J. C., Cafeo, J. A., and Ryne, R. D. (2004). “Combining field data and computer simulations for calibration and prediction.” *SIAM Journal on Scientific Computing*, 26(2), 448–466.

Kennedy, M. C. and O’Hagan, A. (2001). “Bayesian calibration of computer models.” *Journal of the Royal Statistical Society: Series B (Statistical Methodology)*, 63(3), 425–464.

Kiureghian, A. D. and Ditlevsen, O. (2009). “Aleatory or epistemic? does it matter?.” *Structural Safety*, 31(2), 105–112.

Maupin, K. A. and Swiler, L. P. (2020). “Model discrepancy calibration across experimental settings.” *Reliability Engineering and System Safety*, 200, 106818.

Morrison, R. E., Oliver, T. A., and Moser, R. D. (2018). “Representing model inadequacy: A stochastic operator approach.” *SIAM/ASA Journal on Uncertainty Quantification*, 6(2), 457–496.

Oberkampf, W. L., DeLand, S. M., Rutherford, B. M., Diegert, K. V., and Alvin, K. F. (2002). “Error and uncertainty in modeling and simulation.” *Reliability Engineering & System Safety*, 75(3), 333–357.

Pernot, P. (2017). “The parameter uncertainty inflation fallacy.” *The Journal of Chemical Physics*, 147(10).

Plumlee, M. (2017). “Bayesian calibration of inexact computer models.” *Journal of the American Statistical Association*, 112(519), 1274–1285.

Portone, T. and Moser, R. D. (2022). “Bayesian inference of an uncertain generalized diffusion operator.” *SIAM/ASA Journal on Uncertainty Quantification*, 10(1), 151–178.

Qian, P. Z. G. and Wu, C. F. J. (2008). “Bayesian hierarchical modeling for integrating low-accuracy and high-accuracy experiments.” *Technometrics*, 50(2), 192–204.

Quek, A., Ouyang, N., Lin, H.-M., Delaire, O., and Guilleminot, J. (2025). “Enhancing robustness in machine-learning-accelerated molecular dynamics: A multi-model nonparametric probabilistic approach.” *Mechanics of Materials*, 202, 105237.

Roy, C. J. and Oberkampf, W. L. (2011). “A comprehensive framework for verification, validation, and uncertainty quantification in scientific computing.” *Computer Methods in Applied Mechanics and Engineering*, 200(25–28), 2131–2144.

Sargsyan, K., Huan, X., and Najm, H. N. (2019). “Embedded model error representation for bayesian model calibration.” *International Journal for Uncertainty Quantification*, 9(4), 365–394.

Sargsyan, K., Najm, H. N., and Ghanem, R. (2015). “On the statistical calibration of physical models.” *International Journal of Chemical Kinetics*, 47(4), 246–276.

Sirovich, L. (1987). “Turbulence and the dynamics of coherent structures part i: Coherent structures.” *Quarterly of Applied Mathematics*, 45(3), 561–571.

Soize, C. and Farhat, C. (2017). “A nonparametric probabilistic approach for quantifying uncertainties in low-dimensional and high-dimensional nonlinear models.” *International Journal for Numerical Methods in Engineering*, 109(6), 837–888.

Soize, C. and Farhat, C. (2019). “Probabilistic learning for modeling and quantifying model-form uncertainties in nonlinear computational mechanics.” *International Journal for Numerical Methods in Engineering*, 117(7), 819–843.

Strong, M. and Oakley, J. E. (2014). “When is a model good enough? deriving the expected value of model improvement via specifying internal model discrepancies.” *SIAM/ASA Journal on Uncertainty Quantification*, 2(1), 106–125.

Trucano, T., Swiler, L., Igusa, T., Oberkampf, W., and Pilch, M. (2006). “Calibration, validation, and sensitivity analysis: What’s what.” *Reliability Engineering & System Safety*, 91(10–11), 1331–1357.

Tuo, R. and Jeff Wu, C. F. (2016). “A theoretical framework for calibration in computer models: Parametrization, estimation and convergence properties.” *SIAM/ASA Journal on Uncertainty Quantification*, 4(1), 767–795.

Wang, H., Guilleminot, J., and Soize, C. (2019). “Modeling uncertainties in molecular dynamics simulations using a stochastic reduced-order basis.” *Computer Methods in Applied Mechanics and Engineering*, 354, 37–55.

Wang, Z. and Ghanem, R. (2023). “Stochastic modeling and statistical calibration with model error and scarce data.” *Computer Methods in Applied Mechanics and Engineering*, 416, 116339.

Xiao, H., Wu, J.-L., Wang, J.-X., Sun, R., and Roy, C. (2016). “Quantifying and reducing model-form uncertainties in reynolds-averaged navier–stokes simulations: A data-driven, physics-informed bayesian approach.” *Journal of Computational Physics*, 324, 115–136.

Yadav, A. and Zhang, R. (2025a). “Bayesian optimization under uncertainty for training a scale parameter in stochastic models.

Yadav, A. and Zhang, R. (2025b). “Stochastic subspace via probabilistic principal component analysis for characterizing model error.” *Computational Mechanics*.

Zeng, X. and Ghanem, R. (2023). “Projection pursuit adaptation on polynomial chaos expansions.” *Computer Methods in Applied Mechanics and Engineering*, 405, 115845.

Zhang, H., Dolbow, J. E., and Guilleminot, J. (2024). “Representing model uncertainties in brittle fracture simulations.” *Computer Methods in Applied Mechanics and Engineering*, 418, 116575.

Zhang, H. and Guilleminot, J. (2023). “A riemannian stochastic representation for quantifying model uncertainties in molecular dynamics simulations.” *Computer Methods in Applied Mechanics and Engineering*, 403, 115702.

Zhang, R. and Ghanem, R. (2021). “Normal-bundle bootstrap.” *SIAM Journal on Mathematics of Data Science*, 3(2), 573–592.

Zhang, R., Mak, S., and Dunson, D. (2022). “Gaussian process subspace prediction for model reduction.” *SIAM Journal on Scientific Computing*, 44(3), A1428–A1449.

Zou, Z., Meng, X., and Karniadakis, G. E. (2024). “Correcting model misspecification in physics-informed neural networks (pinns).” *Journal of Computational Physics*, 505, 112918.